Instrument Science Report COS 2015-02

Summary of the COS Cycle 20 Calibration Program

Julia Roman-Duval, Alessandra Aloisi, K. Azalee Bostroem, Justin Ely, Stephen Holland, Sean Lockwood, Cristina Oliveira, Steven Penton, Charles Proffitt, David Sahnow, Paule Sonnentrucker, Alan D. Welty, Thomas Wheeler

June 10, 2015

ABSTRACT

We summarize the Cycle 20 calibration program for the Cosmic Origins Spectrograph (COS) on the Hubble Space Telescope, covering the time period from November 2012 through October 2013. We give an overview of the Calibration plan and status summaries for each of the individual proposals comprising the C20 Calibration program.

1. Introduction

The Cosmic Origins Spectrograph (COS) was installed on the Hubble Space Telescope in May 2009. Cycle 20 was thus the fourth cycle of on-orbit operations for COS, running from November 2012 through October 2013. Each cycle, the COS team monitors the performance of the COS instrument through routine calibration programs, which monitor, for instance, the throughput and wavelength calibration of the COS FUV and NUV detectors.

In this document we record and summarize the results of the 18 individual calibration programs that comprise the Cycle 20 calibration plan. Section 2 gives a summary and overview of the calibration plan. In Cycle 20, all 8 calibration programs monitored and tracked instrument performance. There were no special nor contingency calibration programs in Cycle 20. A new program (13124) tracking the performance of COS ACQ/IMAGE target acquisitions was implemented in Cycle 20.

Section 3 details results from the individual calibration programs. The appendix lists reference files produced as a result of Cycle 20 calibration programs.

2. Overview of Cycle 20 calibration programs

Table 1 summarizes the orbit allocation and usage for the regular Cycle 20 calibration program. The calibration monitoring programs in Cycle 20 are essentially continuations of the monitoring programs from the previous cycle. They monitor instrument throughput, dispersion, and performance. Reference files are updated only as-needed to maintain instrument calibration within the required specifications.

Table 1: Orbit allocation and usage during the regular C20 calibration program.

	External Orbits	**Internal Orbits**	**Parallel Orbits**
Allocated	44	313+36[C]	4
Executed	44+2[H]=46	313	4
Withdrawn	0	0	0
Failed	2	0	0
Repeated	2	0	0

[C] Contingency orbits, [H] HOPR

Currently available reference files can be found at the following web address: www.stsci.edu/hst/observatory/cdbs/SIfileInfo/COS/reftablequeryindex. Other products resulting from the calibration program include COS Instrument Science Reports (ISRs), COS Technical Instrument Reports (TIRs), and updates to the COS Instrument (IHB) and Data (DHB) Handbooks. Links to these documents can be found at: www.stsci.edu/hst/cos/documents. Note that TIRs are only available on the internal STScI web site. In order to retrieve TIRs a document request needs to be sent to help@stsci.edu.

Table 2 provides a high-level summary of the calibration programs, noting specifically products and accuracy achieved. The first two columns give the Proposal ID and its title; columns 3 and 4 give the number of executed[allocated] orbits for each proposal, divided into external and internal orbits. Column 5 gives the frequency of visits for monitoring programs. Column 6 describes the resulting products. For several programs, regularly updated reference files are produced. For many others, results are either posted on the web, or simply documented in Section 3 of this report. Column 7 gives the accuracy achieved by the calibration proposal. The last column of Table 2 notes the page in this ISR on which detailed information for that program can be found.

3. Results from individual programs

The following sections summarize the purpose, status, and results from the individual calibration proposals in the Cycle 20 program.

Table 2: High-level summary of the Cycle 20 calibration programs

PID	Title	Orbits used Executed/allocated		Frequency	Products	Accuracy Achieved	Page
		External	Internal				
	NUV Monitors						
13128	COS NUV MAMA Fold Distribution	--	1[1]	Once	Reported in this ISR	<5% on location of peak of fold distribution	4
13126	COS NUV Detector Dark Monitor	--	52[52]	1/week	Reported in this ISR	0.2% in global dark rate uncertainty	7
13125	COS NUV Spectroscopic Sensitivity Monitor	$6+2^{H}$[6]	--	3x1/L, 3x1/M	TDS Reference file	S/N of 30 per resel	9
13127	COS NUV Internal/External Wavelength Scale Monitor	1[1]	--	1x1	Reported in this ISR	1.7-3.7 pixels in wavelength scale accuracy	11
13124	Monitoring of COS ACQ/IMAGE Performance	2[2]	--	1x2	None	0.5 NUV pixel	13
13129	COS NUV recovery after Anomalous Shutdown	--	$0[4^{C}]$	Contingency	None	N/A	--
	FUV Monitors						
13121	COS FUV Detector Dark Monitor	--	260 [260]	5/week	Reported in this ISR	0.1% in global dark rate uncertainty	15
13119	COS FUV Spectroscopic Sensitivity Monitor	33[33]	--	12x2/G140L +G130M, 10x1/G160M	TDS Reference file	S/N of 30 per resel	17
13122	COS FUV Internal/External Wavelength Scale Monitor	2[2]	--	1x2	Reported in this ISR	wavelength scale accuracy 5.7-7.5 pix G130M, 5.8-7.2 pix G160M, 7.5-12.5 pix G140L	21
13123	COS FUV Recovery After Anomalous Shutdown	--	Contingency $0[32^{C}]$	Contingency	None	N/A	--
13145	COS observations of geo-coronal Lyman alpha emission (COS pure parallel)	$4^{P}[4^{P}]$	--	4x1	Reported in this ISR	N/A	23

^{C} Contingency orbits, ^{H} HOPR, ^{P} Parallel orbits

Proposal ID 13128: COS NUV MAMA Fold Distribution (PI: Thomas Wheeler)

Analysis Lead, Others: Thomas Wheeler, Alan D. Welty (CoI)

Summary of Goals and Program Design

The performance of the NUV MAMA microchannel plate can be monitored using a MAMA fold analysis procedure that provides a measurement of the distribution of charge cloud sizes incident upon the anode giving some measure of change in the pulse-height distribution of the MCP and, therefore, MCP gain. The goal is the continued monitoring of the NUV MAMA detector and comparing the results with previous results to detect trends or anomalous behavior. This program is based on Cycle 19 proposal 12723.

Execution

All visits were executed on May 1, 2013.

Summary of Analysis

The engineering telemetry data will be examined (voltages, currents, temperatures, relay positions, and status) for agreement with predicted values and previous ground and on-orbit test data. A MAMA time-tag image data is used to construct a histogram of the number of counts for each fold. The results are compared and combined with the previous test results.

Post test, a dark exposure is taken where the counters are cycled and are plotted in a histogram and compared with earlier results.

No anomalous behavior was detected. The NUV MAMA does exhibit a known high dark count rate caused by widow phosphorescence that has been increasing since installation during SMOV4. Results are sent to the COS/STIS Science Team and V. Argabright of Ball Aerospace for review and comments.

Below is the NUV fold histogram followed by the post-test dark count histogram.

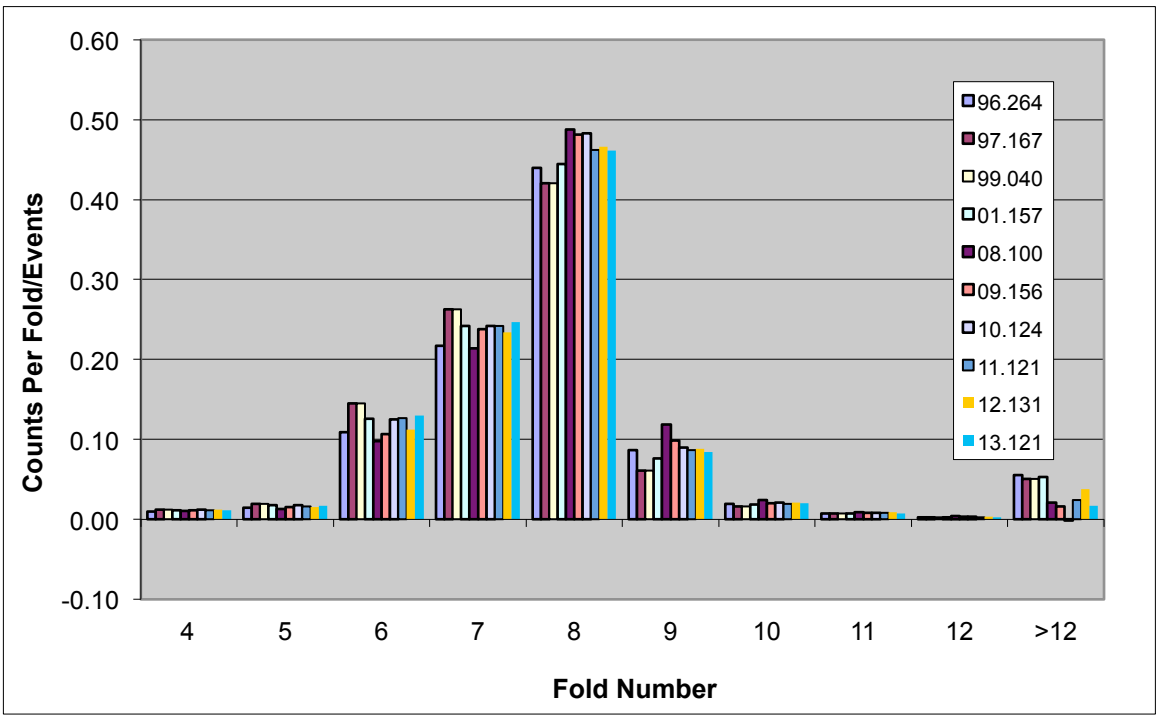

Figure 1. NUV MAMA Fold Histogram

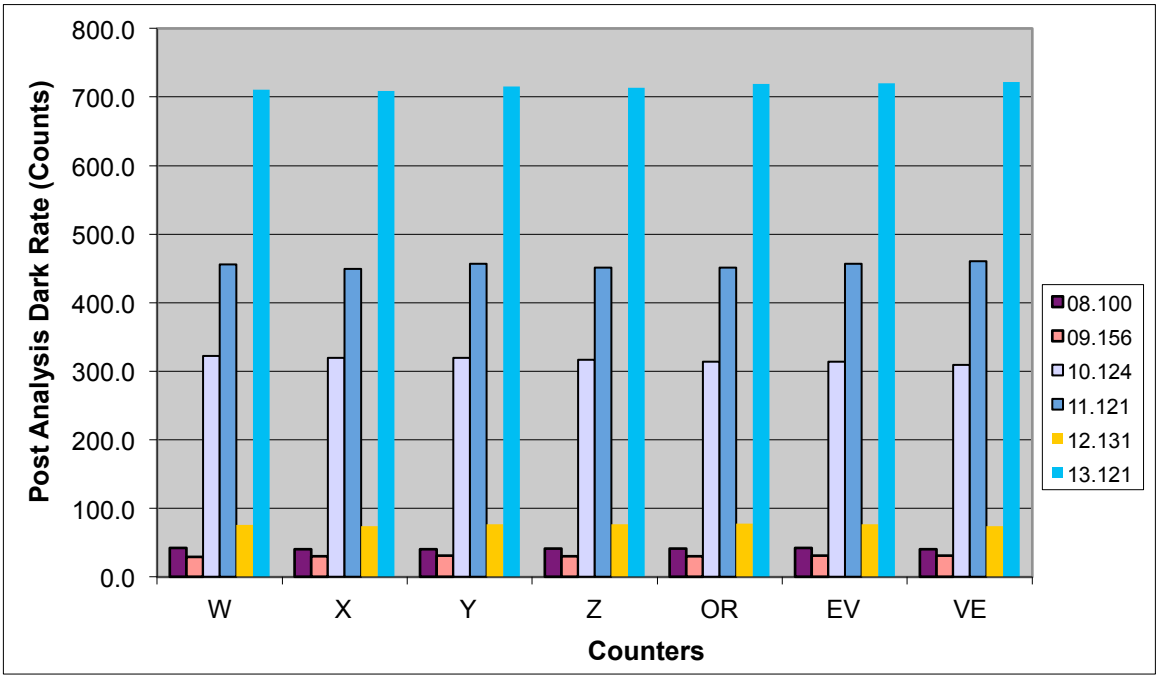

Figure 2. NUV MAMA Post-Test Dark Count Histogram

Accuracy Achieved

Position of the peak in the fold distribution can be measured to about 5% accuracy from this procedure.

Reference Files Delivered

N/A

Relevant ISRs

No ISRs will be published

Continuation Plans

This monitoring program continued in Cycle 21 as Proposal 13531

Supporting Details

None.

Proposal ID 13126: COS/NUV Detector Dark Monitor (PI: Justin Ely)

Analysis Lead, Others: Justin Ely, David Sahnow, Charles Proffitt

Summary of Goals and program design

Perform routine monitoring of the NUV MAMA detector dark rate. The main purpose is to look for evidence of a change in the dark rate, both to track on-orbit time dependence and to check for any developing detector problems. Results from this program are used to update the ETC and the IHB.

Execution

Every two weeks, two 22-minute exposures were taken with the shutter closed for a total of 52 orbits. All observations were successful.

Summary of Analysis and Results

The global dark rate of each observation was measured, and the overall trend was monitored as a function of time. The data, initially fit well with a linear relation, now shows a slower increase with time and larger variability, the latter being induced by temperature and seasonal changes.

Accuracy Achieved

Due to the changing trend with time, we adopt an ETC estimate for the dark-rate that corresponds to the 95% level in the probability distribution function determined from dark measurements over a period of the previous 6 months to 1 year.

Reference Files Delivered

None

Relevant ISRs

None

Continuation Plans

Program continued in Cycle 21 as 13528.

Supporting Details

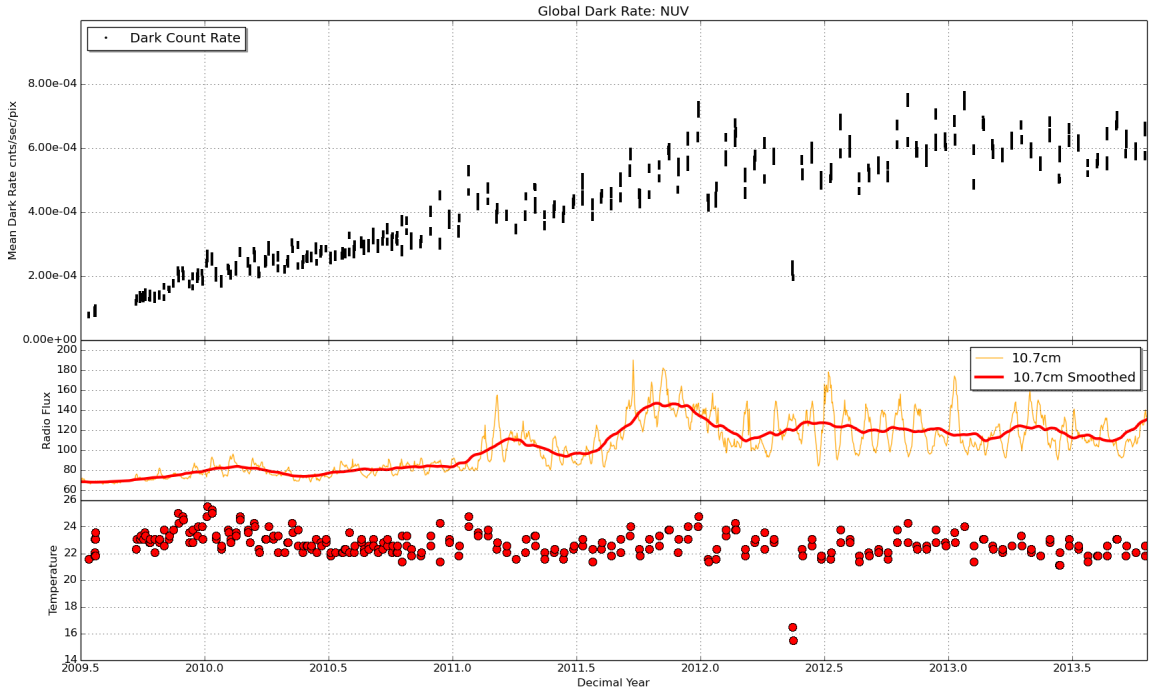

Figure 3. COS NUV dark rate as a function of time, from the COS installation through Cycle 20. The first subplot shows the measured dark-rate in 25 second increments throughout every observation. The groupings of points represent individual exposures, and demonstrate that the variability within a given exposure is low. The middle subplot displays the 10.7 cm radio flux used to track the solar cycle, and the last subplot displays the detector temperature for each observation.

Proposal ID 13125: NUV Spectroscopic Sensitivity Monitor (PI: K. Azalee Bostroem)

Analysis Lead, Others: K. Azalee Bostroem

Summary of Goals and program design

Monitor the sensitivity of each NUV grating to detect changes due to contamination or other causes. Characterize these changes as a function of wavelength, grating, and stripe and update the time-dependent sensitivity reference file, if necessary, for use with pipeline flux calibration.

Due to sensitivity differences on the medium- and low- resolution gratings, two spectrophotometric white dwarf standard star targets are used in this monitoring: WD1057+719 for G230L, and G191B2B for G185M, G225M, and G285M.

As trends have been stable over the last 3 cycles we reduced the monitoring from 4 times per year to 3 times per year.

Execution

This program was allocated 6 orbits and should have executed every 4 months. The first set of visits, L1 and M1, executed nominally on December 9, 2012 and the third set of visits, L3 and M3, executed nominally on September 22, 2013. However, the L2 and M2 visits were affected by an error in the flight software caused the spectroscopic target acquisition to fail. COS observations using a spectroscopic target acquisition were suspended until the installation of a flight software LV52 on 07/8/2013. Visits L2 and M2 were repeated as visits L4 and M4 on July 26, 2013.

Summary of Analysis and Results

The computation of the time-dependent sensitivities for COS NUV data from previous cycles is described in Osten et al. (2010; COS ISR 2010-15) and Osten et al. (2011; COS ISR 2011-02). The same analysis techniques and code used in previous cycles are used in Cycle 20. Figure 4 summarizes the behavior of the spectroscopic sensitivity through October 2013. The G230L and G185M gratings, which have a MgF_2 coating, exhibit slightly increasing sensitivity trends with slopes between -0.5 – 1.0 %/yr. The positive trends in the G185M grating appear to have reversed in late 2011 and so these trends should be fit by a piecewise linear trend in the future. It does not appear that the trend has turned over in the G230L grating. The bare-Al gratings (G225M and G285M), which have exhibited sensitivity declines from the beginning of Cycle 17, continue to decline at a steady rate of 2.3 – 3.0%/yr and 11.9 – 12.0%/yr respectively. These values are consistent with the results from pre-launch grating efficiency tests. The wavelength dependence of the G285M and the shortest wavelengths of G225M continues in this cycle with the same trends.

Accuracy Achieved

Phase I accuracy of S/N = 30 was achieved for G185M, G225M, and G230L. The required accuracy of S/N = 26 in the G285M was not achieved. The G285M/2617

setting achieved S/N = 25.1 in the first visit and S/N = 23 in the last visit. The G285M/3094 setting achieved S/N = 23.5 in the first visit and S/N = 21.5. All S/N ratios are quoted at the central wavelength and per resolution element (3 pixels).

Reference Files Delivered

None

Relevant ISRs

None

Continuation Plans

The program continued in Cycle 21 as 13527. No changes were made.

Supporting Details

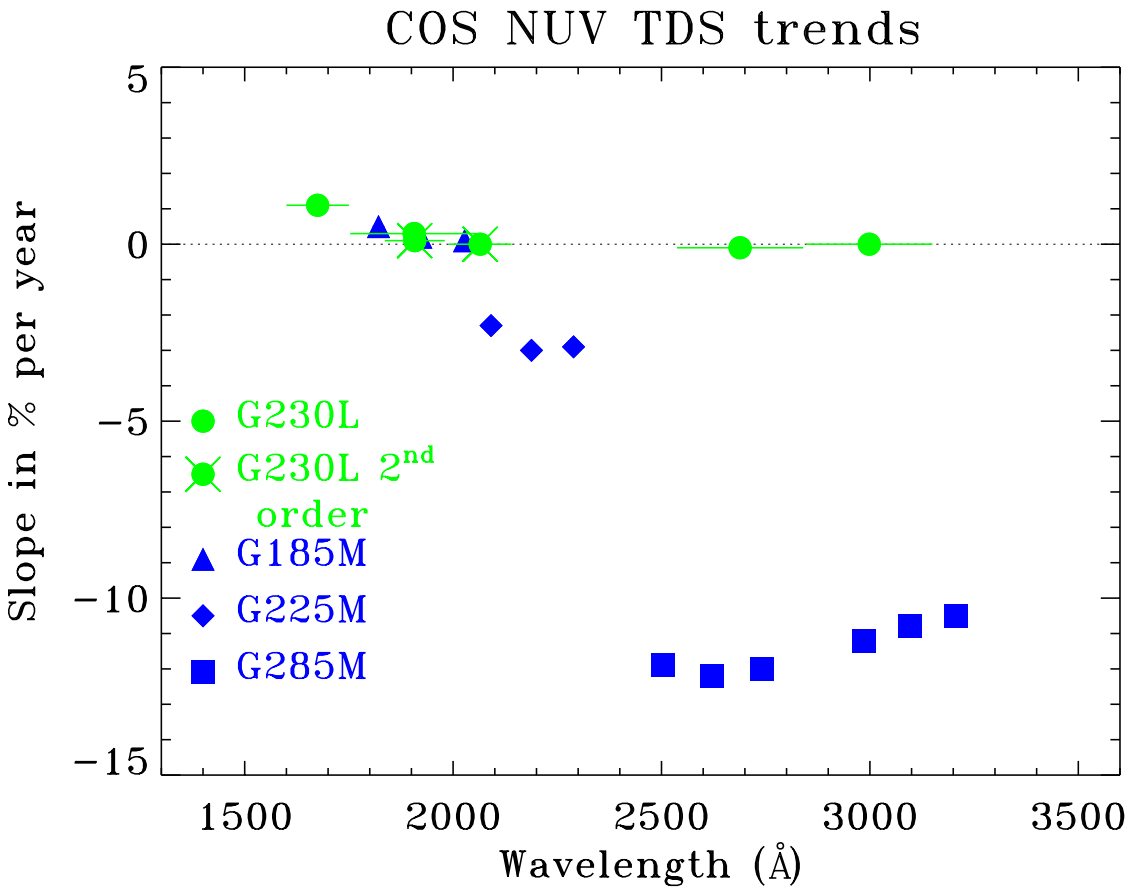

Figure 4. NUV TDS slope as a function of wavelength for different NUV gratings. Slopes are calculated based on all NUV TDS monitoring data acquired since SMOV4.

Proposal ID 13127: COS NUV Internal/External Wavelength Scale Monitor (PI: Paule Sonnentrucker)

Analysis Lead, Others: Paule Sonnentrucker

Summary of Goals and program design

This program monitors the offset between the internal and external wavelength scales. This offset is referred to as "DELTA" in the wavelength dispersion solution reference file and corrects for the shift between the WCA and PSA in TV03 versus the shift between the WCA and PSA on orbit: $(WCA - PSA)_{TV03} - (WCA - PSA)_{orbit}$. Analysis of TV data indicates that this DELTA (offset) is cenwave and FP-POS independent for a particular grating, but it is grating and stripe dependent. To monitor this effect, we observed selected cenwaves for all NUV gratings.

Execution

The program executed as a one-orbit visit on August 2nd, 2013 shortly after the move of operations to lifetime position 2. The wavelength scales of the following settings were monitored G185M/2010, G225M/2217, G285M/2676, and G230L/2635/2950/3000 (all at FP- POS=3) using external target HD6655.

Summary of Analysis and Results

For spectra that overlap with STIS E230M data of HD6655, shifts between the COS and STIS ISM lines were measured for each setting. These shifts, or offsets, are listed in Table 3 in units of pixel. For those settings that have no overlap with the STIS E230M data, shifts were measured relative to the third epoch of Cycle 19 COS monitoring program 12722 (V03; execution Sept 2012). These offsets are listed in Table 4.

Accuracy Achieved

The COS specifications for NUV wavelength accuracies are 1.7 – 2.4 pix for G185M, 2.3 – 3.2 pix for G225M, 2.3 – 3.5 pix for G285M, and 2.0 – 3.7 pix for G230L. The results given in Table 3 seem to indicate that there is a systematic offset, of +1 to ~ +4 pix between the zero point of the COS/NUV and STIS/E230M wavelength scales. There are in addition small variations of the zero point of the COS wavelength scale, which are within the accuracies given above when comparing the Cycle 20 data with Cycle 19 data taken at a similar epoch. In all cases, the required accuracy is achieved within errors (0.5 pixels). We might want to consider updating the reference file zero-point offset for some gratings.

Reference Files Delivered

N/A

Relevant ISRs

Details are included in a multi-cycle ISR by Sonnentrucker et al. (2015, in prep)

Continuation Plans

This program was continued in Cycle 21 under PID 13529. Three monitoring visits of 1 orbit each were scheduled to execute every ~4 months.

Supporting Details

Table 3. Offsets in pixels that need to be applied to shift the COS/NUV spectral lines of HD 6655 so that they align with the STIS E230M spectral lines (reference) of the same target. For G230L spectra, stripe C contains mostly second order light. Stripe A covers wavelengths shorter than ~ 2100 Å. For both of these stripes there is no overlap with the wavelength range of the STIS E230M data. The same applies to stripes A and B of G225M/2217 and all the stripes of G185M/2010. The data were taken on August 2nd, 2013.

Visit	Stripe	G225M 2217	G285M 2676	G230L 2635	G230L 2950	G230L 3000
Aug. 2, 2013	A B C	... … +3.8	+2.3 +2.1 +2.7	… +1.1 …	… +3.0 …	… +1.3 …

Table 4. Offsets in pixels between the Cycle 20 COS/NUV spectra of HD 6655 (Visit 01; P13127) and the Cycle 19 COS/NUV spectra (Visit 03; P12722; reference) for all settings with adequate S/N ratios.

Visit	Stripe	G185M 2010	G225M 2217	G285M 2676	G230L 2635	G230L 2950	G230L 3000
Aug. 2, 2013	A B C	... +1.3 +1.9	+1.0 +1.2 +0.9	+0.9 +1.4 +1.2	… +1.0 …	… +1.3 …	… +1.3 …

Proposal ID 13124: Monitoring of ACQ/IMAGE performance (PI: Steven Penton)

Analysis Lead, Others: Steven Penton

Summary of Goals and program design

This program was designed to check several parameters related to COS target acquisition (TA). The first goal was to test the co-alignment of the four COS ACQ/IMAGE modes (PSA+MIRRORA, PSA+MIRRORB, BOA+MIRRORA, and BOA+MIRRORB). The second goal was to check the "WCA-to-PSA" and "WCA-to-BOA" offsets for all COS NUV and FUV gratings.

The co-alignment of PSA+MIRRORA and PSA+MIRRORB is actually obtained in a separate program (13171). This program (HST Cycle 20 Focal Plane Calibration (SI-FGS Alignment, PI=Cox), executes every six months as a part of the Science Instrument (SI) to Fine Guidance Sensor (FGS) alignment check.

Program 13124 consists of three visits. The first visit begins with a co-alignment check of PSA+MIRRORB to BOA+MIRRORA ACQ/Images. After this check, the WCA-to-PSA offsets are checked for G230L/3000, G285M/2850, G130M/1309. The second visit was executed on a second, brighter target, This visit begins with a co-alignment check of the BOA+MIRRORA to BOA+MIRRORB ACQ/Images. After this imaging alignment check, the WCA-to-PSA offsets are checked for G185M/1890, G225M/2306, G160M/1623 and the WCA-to-BOA offset for G160M/1623. All spectroscopic exposures were taken of FPPOS=3, as this is the FPPOS used during target acquisition.

A third visit of 13124 was prepared as a contingency visit in the case of a problem with the execution of Visit 02 of 13171, but it was not executed.

Execution

The 13171 visit (02) executed on Sept 1, 2013. Visit 01 of 13124 executed on Oct 24, 2013 and Visit 02 of 13124 executed on Nov 1, 2013. All observations were successful.

Summary of Analysis and Results

The ACQ/Images showed that the imaging TA modes were co-aligned to about 2 NUV pixels, which equates to about 0.05". This was much larger than expected as in SMOV, these channels were co-aligned to better than 0.5 pixels (0.01"). The strictest NUV TA accuracy requirement is for the G185M, which is 0.058", the measured error in co-alignment between the imaging modes. The strictest FUV centering TA requirement is for G130M, which is 0.150".

At the time, the cause of the ACQ/Image mis-alignment was unknown. Subsequent analysis in 2014 indicated that drift in OSM 1 and OSM 2, combined with the increasing background rate of the NUV channel was causing the centering of the MIRRORB exposures to be different from that of SMOV. No adjustments were made to the ACQ/Image MIRRORB WCA-to-PSA/BOA offsets based solely upon the data of this program.

Based upon the data of 13124, the WCA-to-PSA offsets for the NUV gratings was not changed, even though some of the offsets appeared to off. The uncertainty of why the ACQ/Image modes were not co-aligned precluded the use of this data for these purposes.

Accuracy Achieved

Imaging WCA-to-SA offsets need to be known to better than 0.5 NUV pixels in both dispersion and cross- dispersion (XD). Spectroscopic WCA-to-SA offsets need to known to 0.5 XD pixel. These goals were achieved with the data of this program.

Reference Files Delivered

No reference files were delivered, but the data in this program was used to justify the adjustment of all FUV LP2 WCA-to-PSA and WCA-to-BOA offsets due to gain sag (and therefore Y-walk) at LP2. On May 27, 2014, all FUV WCA-to-PSA and WCA-to-BOA offsets were increased (more negative) by -1.5 FUV rows. This change occurred as the FSW release LV55.

Relevant ISRs

No ISRs were produced from this program.

Continuation Plans

This program is to continued annually, with the Cycle 21 program being 13526. Based upon experience from this program, the BOA exposure was removed from this program for 13526. That program replaced the BOA exposure with two exposures placed at +/- 0.7" from the nominal position. These exposures will provide additional information which will be helpful in tracking future Ywalk and gain sag

Supporting Details

None

Proposal ID 13121: COS/FUV Detector Dark Monitor (PI: Justin Ely)

Analysis Lead, Others: Justin Ely, David Sahnow

Summary of Goals and program design

Perform routine monitoring of FUV XDL detector dark rate. The main purpose is to look for evidence of a change in the dark rate, both to track on-orbit time dependence and to check for a developing detector problem. Results from this program are used to update the ETC and the IHB.

Execution

Every week, five 22-minute exposures were taken with the shutter closed for a total of 260 orbits. All observations were successful.

Summary of Analysis and Results

After screening for SAA passages, the dark rate of each observation was measured in 25 second intervals from a region that excluded the noisy edges of the active area. Dark rates were measured vs. time and summed darks for each visit were constructed from all non- SAA impacted events.

As shown in Figure 5, the overall trend in the dark rate has been relatively constant for Segment B, while Segment A appears to have experienced a persistent baseline increase in late 2011 through most of 2012 and again midway through 2013. The more recent jumps show two discrete events; both exhibiting an initial increase followed by settling into a new baseline value.

Additionally, both segments show individual observations and portions of observations that significantly vary from the baseline dark rate. Both of these effects appear to have some correlation with the solar cycle, though direct cause and effect have not yet been determined.

Accuracy Achieved

Due to the lack of a measureable trend and the extreme variability seen in observations, we adopt an ETC estimate for the dark-rate that corresponds to the 95% level in the probability distribution function determined from dark measurements over a period of the previous 6 months – 1 year.

Reference Files Delivered

None

Relevant ISRs

None

Continuation Plans

Program continued in Cycle 21 as 13521.

Supporting Details

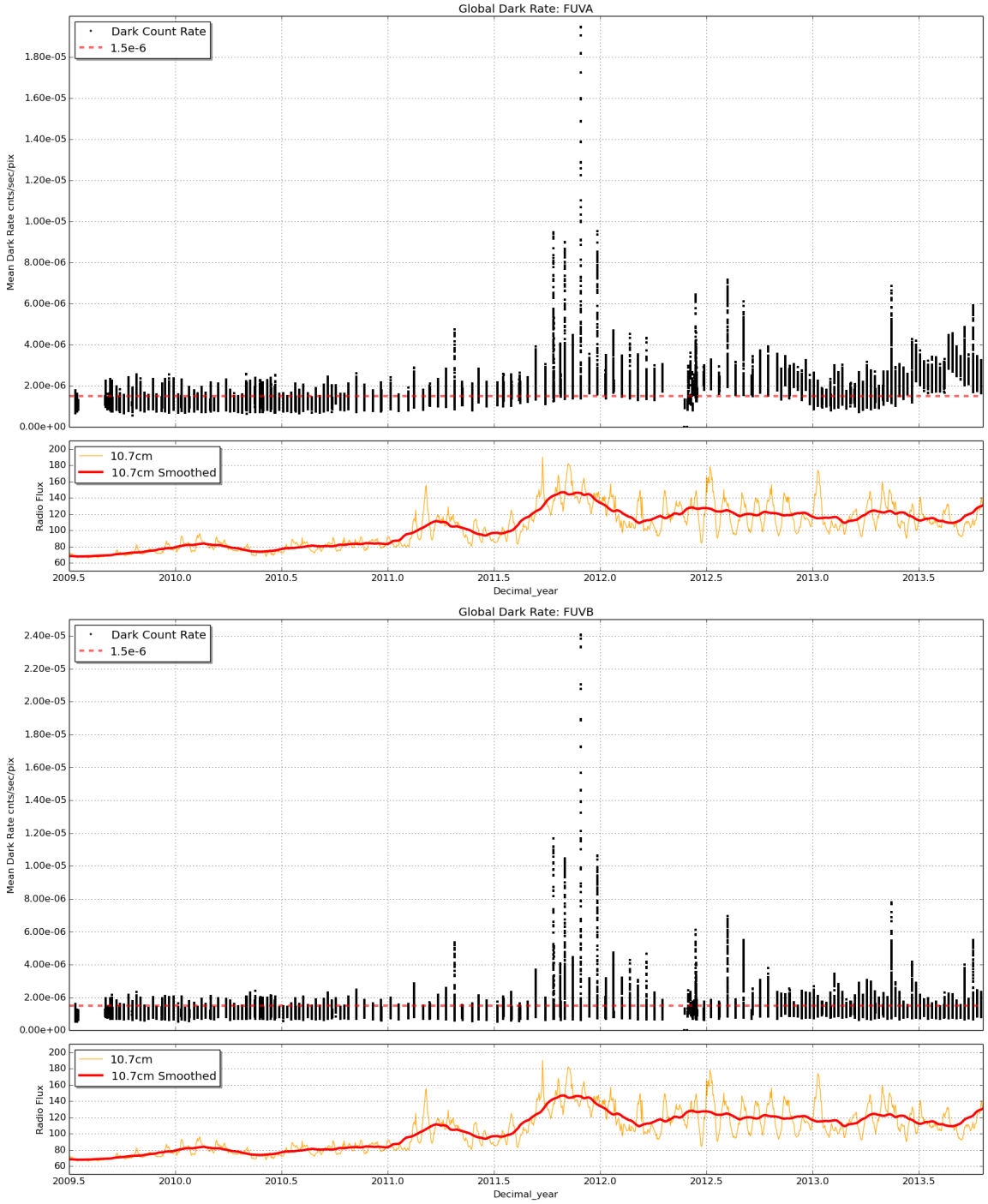

Figure 5. COS/FUV dark rates on FUVA (top) and FUVB (bottom) as a function of time, from COS installation through Cycle 20. For each panel the top plots show the measured dark-rate in 25 second increments throughout every observation. The groupings of points represent individual visits, and demonstrate that the variability within a given exposure is sometimes extremely large. The red dashed line displays a fiducial dark rate of 1.5×10-6 cts/pix/s. For each panel the bottom plots display the 10.7 cm emission tracking the solar cycle.

Proposal ID 13119: COS FUV Time-Dependent Sensitivity (PI: K. Azalee Bostroem)

Analysis Lead, Others: K. Azalee Bostroem

Summary of Goals and program design

Monitor the sensitivity of each FUV grating to detect changes due to contamination or other causes. Characterize these changes as a function of wavelength, grating, and segment, and update the time-dependent sensitivity reference file, if necessary, for use with pipeline flux calibration. Exposure times are set to obtain a signal to noise ratio (SNR) of 15 at the wavelength of *least* sensitivity except for modes G130M/1055, G130M/1096, G140L/1055, and G140L/1280 where the sensitivity falls off steeply towards shorter wavelengths. Exposure times for the G130M/1055 and 1222 are chosen to reach a SNR of 25 at the wavelength of *most* sensitivity.

Two white dwarf standard stars are used to monitor the FUV TDS in Cycle 20: WD0308-565 and GD71. The target used to monitor each mode is detailed in Table 5 and are chosen to optimize the SNR of the mode while minimizing the impact of the monitoring on the detector lifetime.

Table 5. The target used to monitor different COS FUV modes (grating/central wavelength/detector)

Grating	Central Wavelength	FUVA Target	FUVB Target
G130M	1096	GD71	GD71
	1222	WD0308-565	WD0308-565
	1291	WD0308-565	WD0308-565
	1327	WD0308-565	WD0308-565
G160M	1577	GD71	WD0308-565
	1623	GD71	WD0308-565
G140L	1105	WD0308-565	GD71
	1280	WD0308-565	WD0308-565

There are no wavelength calibration lamp lines available on the wavelength range covered by G130M/1096/FUVB. This was realized after the execution of Visits 1-6. Visits 7-9 include a lamp observation with FUVA taken after the science observation with FUVB and before any OSM movement.

Execution

The GO wavecals taken with central wavelength 1096 are labeled as iwave due to an error in TRANS. These are spectroscopic observations. The TRANS error was fixed with PR 77724.

Summary of Analysis and Results

All observations were analyzed using the *cos_tds_analysis.py* script as described in Bostroem (COS TIR 2014-05). The net counts spectrum is binned into 5/20 Å bins for the medium/low resolution modes, respectively. The data taken with the second

set of targets (WD0308-565 and GD71) are scaled to match the original targets using the data from program 12806. A trend is fit to LP1 and scaled LP2 data and the final relation is scaled such that the fit is 1 at 2003.77. The analysis uses breakpoints of 2010.2, 2011.2, 2011.75, 2012.0, and 2012.8. A summary plot of the sensitivity vs time for each segment and solar activity directed towards Earth (Figure 6) is also created using the *make_solar_cycle_plot.py* program.

Slopes for Cycle 20 are very shallow; less than -5%/yr for all wavelengths with positive trends of 0-1 (flat or increasing sensitivity) for FUVB. The positive trends are exaggerated by a discontinuous jump in sensitivity when the voltage was raised on FUVB on June 24, 2013. These trends are summarized in Table 6 and Figure 7.

Table 6. Trends for each grating and segment. The values shown are the maximum and minimum values for all central wavelengths observed with a given grating.

Grating	Slope FUVA	Slope FUVB
G130M	-5.1 – +0.4	-0.9 – +2.1
G160M	-3.1 – +0.1	-1.3 – +2.9
G140L	-3.3 – +3.7	-0.5

A new TDS reference file was delivered in September 2013 where all slopes after 2012.8 are set to 0. While the tools were not yet built to create a reference file from the fit trends, the slopes were sufficiently close to zero that this approximation greatly improved the accuracy of the flux calibration for data taken in Cycle 20.

Accuracy Achieved

For the standard modes a SNR of 15 at the wavelength of least sensitivity is reached with the exception of G140L FUVA whose sensitivity is extremely low at the long wavelength edge. For G140L FUVA the SNR < 15 for wavelengths greater than 1840 Å. The blue modes (1096 and 1222) achieve the required signal to noise ratio of 25 at the wavelength of most sensitivity.

Reference Files Delivered

x9h1254fl_tds.fits

Relevant ISRs

None

Continuation Plans

This program continued in Cycle 21 as program 13125. The monitoring was reduced to monitor all central wavelengths every 2 months and only G130M/1291, G140L/1280, and G160M/1623/FUVB on the alternating months. G130M/1055/FUVA was also added to cover the wavelength gap between G130M/1096/FUVB and G130M/1222/FUVB.

Supporting Details

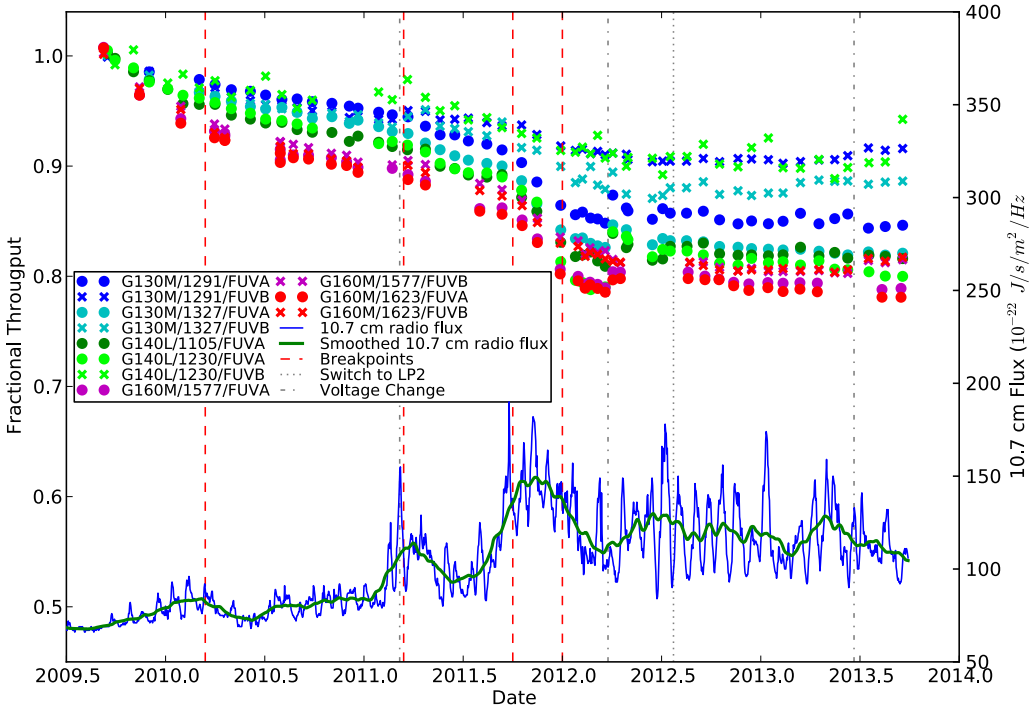

Figure 6. The decline in sensitivity over time (symbols) compared to the solar activity directed at Earth as tracked by 10.7 cm flux (blue solid lines). The dashed red vertical lines represent breakpoints, the dotted grey vertical line marks the move to lifetime position 2 (and the new targets), and the dot-dashed grey vertical lines correspond to changes in the operational voltage on FUVB in 2011 and 2013 and FUVA in 2012. The blue line plots the raw solar cycle data which is smoothed and plotted in green to more easily see the trends. While solar activity has remained high in Cycle 20, the sensitivity trends are shallow indicating a more complicated relationship between solar activity and sensitivity decline than previously thought.

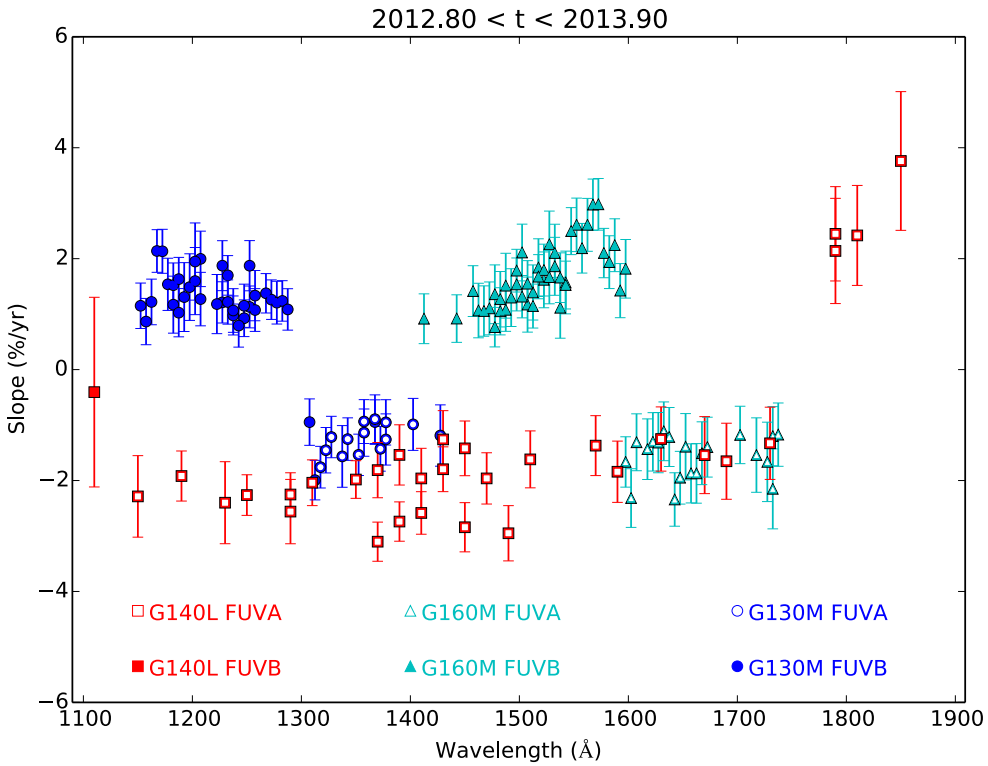

Figure 7. Slope in percent per year as a function of wavelength for the different gratings during Cycle 20. FUVA is plotted as open symbols and FUVB as closed symbols. G130M is represented with blue circles, G160M with cyan triangles, and G140L with red squares. The variation in trend from segment to segment within a grating is apparent.

Proposal ID 13122: COS FUV Internal/External Wavelength Scale Monitor (PI: Paule Sonnentrucker)

Analysis Lead, Others: Paule Sonnentrucker

Summary of Goals and program design

This program monitors the offset between the internal and external wavelength scales. This offset is referred to as "DELTA" in the wavelength dispersion solution reference file and corrects for the shift between the WCA and PSA in TV03 versus the shift between the WCA and PSA on orbit: $(WCA - PSA)_{TV03} - (WCA - PSA)_{orbit}$. Analysis of TV data indicate that this DELTA (offset) is cenwave and FPPOS independent for a particular grating, but it is grating dependent. To monitor this effect, this calibration program observes some cenwaves at different FP-POS positions for all gratings.

Execution

This program is comprised of one visit of 2 orbits to monitor the wavelength scales of the G130M, G160M and G140L gratings using the external SMC target AV75. V01 executed successfully on March 16, 2013. All cenwaves for G140L and the extreme cenwaves for G130M and G160M were observed. Alternate FP-POS positions were used for the M gratings to mitigate gain-sag effects. FP-POS=3 was used for G140L.

Summary of Analysis and Results

Archival STIS E140M data were used to perform a cross-correlation analysis against the COS G130M, G160M and G140L data following the procedure described in Sonnentrucker et al. 2013 (ISR 2013-06). The offsets, in pixel, of the COS ISM lines relative to the STIS E140M data resulting from the cross-correlation analysis are reported in Table 7 and displayed Figure 8.

Accuracy Achieved

The offsets measured are within the 1σ error goals for the COS/FUV wavelength scales, of 5.7-7.5 pix for G130M, 5.8-7.2 pix for G160M, and 7.5-12.5 pix for G140L (see Oliveira et al. 2010, ISR 2010-06)

Reference Files Delivered

N/A

Relevant ISRs

Multi-cycle analysis and results will be reported in ISR (Sonnentrucker et al. 2015 in prep)

Continuation Plans

This program continued in Cycle 21 under program ID 13522 for a total of 2 orbits. The G130M/1096 and G130M/1222 configurations have been added to the monitoring program as these modes are now offered routinely to the community.

Supporting Details

Table 7. Offset range returned by the cross-correlating of COS x1dsum spectra with STIS E140M data for the external target AV75.

Target	Grating	Offset range (pixel)
AV75	G130M	-2.7, +3.3
AV75	G160M	-2.5, +6.7
AV75	G140L-1280	-5.8, +2.0
AV75	G140L-1105	-4.1, +3.9

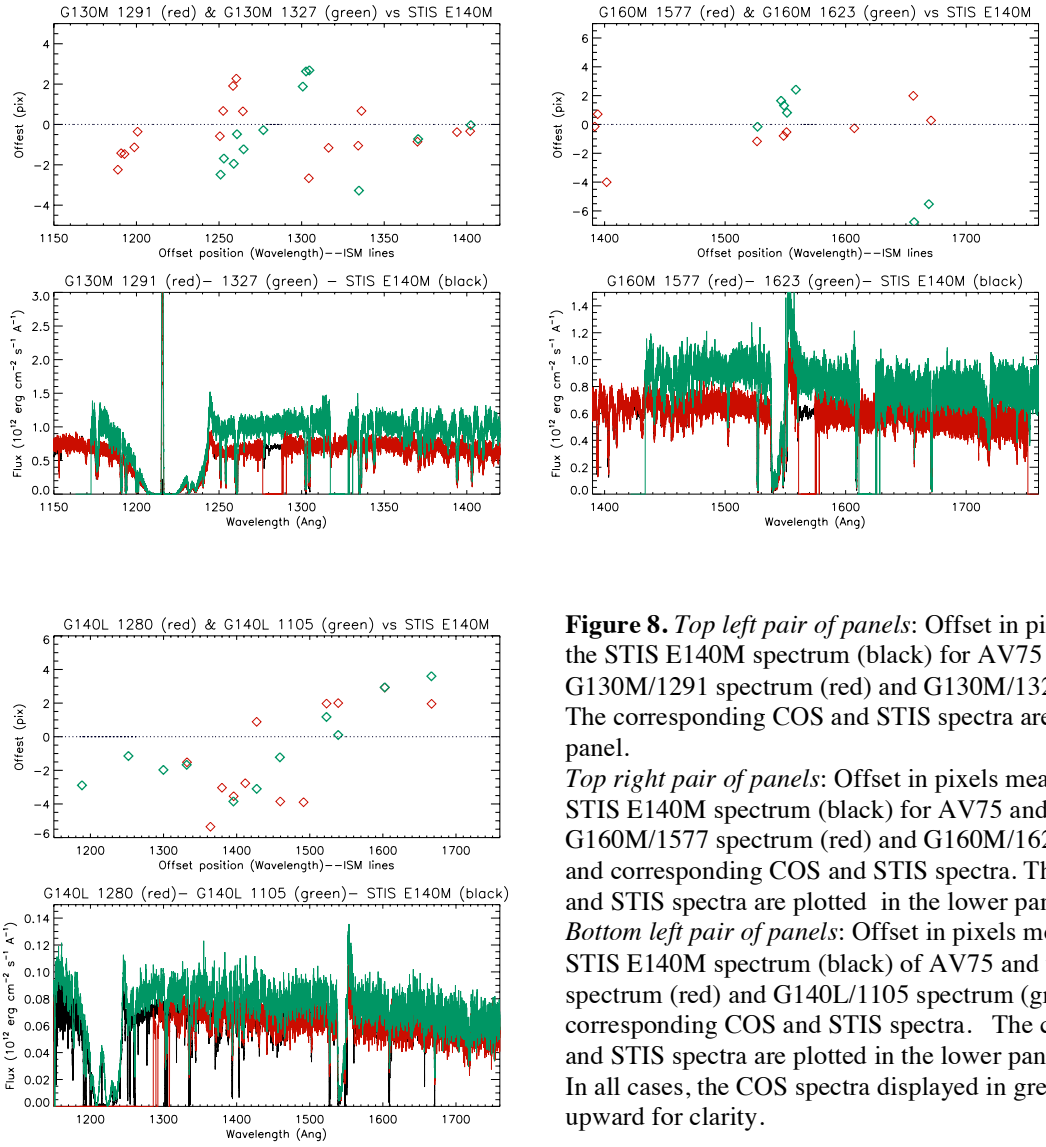

Figure 8. *Top left pair of panels*: Offset in pixels measured between the STIS E140M spectrum (black) for AV75 and the COS G130M/1291 spectrum (red) and G130M/1327 spectrum (green). The corresponding COS and STIS spectra are plotted in the lower panel.
Top right pair of panels: Offset in pixels measured between the STIS E140M spectrum (black) for AV75 and the COS G160M/1577 spectrum (red) and G160M/1623 spectrum (green) and corresponding COS and STIS spectra. The corresponding COS and STIS spectra are plotted in the lower panel.
Bottom left pair of panels: Offset in pixels measured between the STIS E140M spectrum (black) of AV75 and the G140L/1280 spectrum (red) and G140L/1105 spectrum (green) and corresponding COS and STIS spectra. The corresponding COS and STIS spectra are plotted in the lower panel.
In all cases, the COS spectra displayed in green were shifted upward for clarity.

Proposal ID 13145 [COS Pure Parallel]: COS Observations of Geocoronal Ly-α Emission (PI: S. Lockwood)

Analysis Lead, Others: Sean Lockwood, Stephen Holland

Summary of Goals and Program Design

We attempted to collect >10,000 s of geocoronal emission line data with COS on an empty patch of sky. This allowed us to provide the user community with a list of these observations for independent calibration purposes. The previous program (12775) collected shorter integrations on both G130M/1291 and G140L/1105 in 3 visits. We made our observing strategy more efficient to collect the necessary data at lifetime position 2. We succeeded in collecting 11,260 s of G130M/1291/LP2 geocoronal airglow data in this program. Data products were not produced beyond the standard pipeline products, but the datasets were included on the COS Airglow website for utilization by the COS user community.

Execution

Observations were scheduled as pure parallels with 4 STIS monitoring visits. LC4KE2060 in visit E2 truncated early at 2560 s instead of the desired 2900 s.

Summary of Analysis and Results

The data were inspected for anomalies and nothing was identified.

Accuracy Achieved

N/A

Reference Files Delivered

N/A

Relevant ISRs

N/A

Continuation Plans

Continued in Cycle 21 in program 13548. The central wavelength setting was switched from 1291 to 1327 to explore detector position-dependence on the line shapes.

Supporting Details

The list of observations was updated at:
http://www.stsci.edu/hst/cos/calibration/airglow.html

Appendix

Table 8 lists the COS reference files delivered as part of analysis of data taken in COS Cycle 20 calibration programs.

Table 8. Only one reference file was delivered as a result of the Cycle 20 calibration programs.

Reference File	File Type	Delivery Date	Programs Included
x9h1254fl_tds.fits	Time dependent sensitivity	09/19/2013	11897, 12424, 12715, 13119